AMATH 882

Anticipating Critical Transitions in Continuous Bioprocesses

Tom Bury

April 30, 2017

Abstract

Continuous bioprocesses exhibit a range of complex dynamics depending on their internal reaction structure. Multistability often arises as a consequence of positive feedback loops, creating threshold values where abrupt, irreversible transitions may occur. The precise location of these thresholds is hard to determine, and so alternate methods are required to prevent unwanted transitions. We propose statistical indicators from dynamical systems theory, as a tool for anticipating state transitions in these systems. In a preliminary investigation, we confirm their validity for two simple bioprocess models and speculate their application to control and optimisation of bioprocesses on the industrial scale.

1 Introduction

For many years, mathematical models have been used for the design, control and optimisation of continuous bioprocesses [1]. Due to non-linear reaction rates, these processes can exhibit complex dynamical behaviour, such as multistability, oscillations and chaos [2]. Modelling from a dynamical systems perspective, thus provides insight into the type of behaviour that a particular system can exhibit, where much work has been devoted to classifying the behaviour of unstructured bioprocess models [3].

In this paper, we are interested in bioprocesses that exhibit multistability, i.e. the existence of multiple stable states for the same set of parameter values. These systems often possess 'tipping points', that mark a qualitative change in system structure. In a dynamical system framework, these tipping points correspond to bifurcations [4]. Crossing certain types of bifurcation[1] induces a positive feedback causing a dramatic shift in the system state. These shifts, coined 'critical transitions', have become an area of intense study following the proposal of generic early warning signals of their approach [5].

Early warning signals (EWS) for critical transitions arise as a consequence of a universal property of continuous systems. That is, as a critical transition is approached, the rate of return to equilibrium following a small perturbation slows down [6]. This is commonly referred to as 'critical slowing down' [4]. Under the influence of external noise, this causes the system to fluctuate further from equilibrium in a more correlated fashion, which can be detected in a time-series as an increase in variance and autocorrelation [5]. These statistical measures are the most commonly used EWS for an upcoming critical transition.

To date, EWS have proven useful a useful tool for disciplines including ecology, epidemiology, climatology and others. We refer the reader to [5] for an excellent introduction to EWS, and to [7] for a more critical review on their limitations. Arguably, the three most important system requirements for reliable EWS are low observation error, high frequency data, and weak environmental noise. As well as satisfying these conditions, bioprocesses can be set up in the lab for repeated experiments; a luxury that one does not have in the aforementioned fields. For these reasons, we are optimistic that EWS could play an important role in the monitoring and control continuous bioprocesses.

In this paper, we test the EWS of increasing variance and autocorrelation in two simple bioprocess models exhibiting critical phenomena.

[1] the fold bifurcation is a well-known example and appears in most bistable systems

2 Models and Methods

In this section, we outline two prototype models for continuous bioprocesses and their stability properties. Methods for calculating EWS follow.

2.1 Model I : The Haldane Model

The Haldane model considers a continuous feed of substrate into a CSTR, that is utilised for cell growth and product synthesis. The process is described by the system of mass balance equations

$$\frac{dS}{dt} = D(S_f - S) - \sigma(S,P)X, \tag{2.1}$$

$$\frac{dX}{dt} = \mu(S,P)X - DX, \tag{2.2}$$

$$\frac{dP}{dt} = \epsilon(S,P)X - DP, \tag{2.3}$$

where state variables and parameters are described in Table 1. This setup has been shown to capture the behaviour of a number of bioprocesses [8, 9], and is appealing to study for its simplicity. The dilution rate D is the rate at which pure substrate is fed in, and mixture is extracted from, the CSTR. This serves as the control variable that ideally, is adjusted to optimise product output, $\Psi = DP$.

Notation	Definition
S	Limiting substrate concentration $(mass/vol)$
X	Cell biomass concentration $(mass/vol)$
P	Product concentration $(mass/vol)$
D	Dilution rate $(time^{-1})$
S_f	Substrate concentration in the feed $(mass/vol)$
σ	Cell utilisation rate of the limiting substrate $(time^{-1})$
μ	Cell growth rate $(time^{-1})$
ϵ	Cell product formation rate $(time^{-1})$

Table 1: Symbol definitions for the Haldane Model

We adopt the growth rates

$$\sigma(S,P) = a\epsilon(S,P), \tag{2.4}$$

$$\mu(S,P) = \left(\frac{\mu_1 S}{K_{1S} + S + \frac{S^2}{K_{1I}}}\right)\left(\frac{K_{1P}}{K_{1P} + P}\right), \tag{2.5}$$

$$\epsilon(S,P) = \left(\frac{\mu_2 S}{K_{2S} + S + \frac{S^2}{K_{2I}}}\right)\left(\frac{K_{2P}}{K_{2P} + P}\right), \tag{2.6}$$

as used in [3], which are based on the well-known Haldane substrate inhibition kinetics [9]. At low substrate levels, growth rates increase in a near-linear fashion with S, however, excess substrate beyond a critical concentration becomes inhibitory to cell growth (see Figure 1). These forms also assume high levels of product in the tank to be inhibitory.

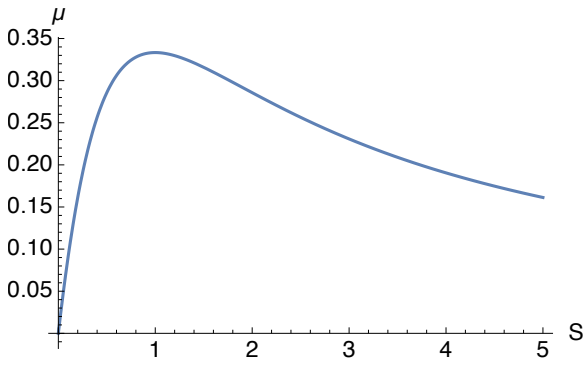

Figure 1: Cellular growth (μ) dependence on substrate concentration (S) for a fixed product concentration.. Approximate linear growth for low levels of substrate, but beyond a critical concentration, higher levels of substrate inhibit growth due to 'wash-out' effects.

This model has been fully analysed in [3], where various parameter regimes have been classified based on the resulting stability structure of the sytstem. We use parameter values of a rescaled model (Appendix A.1), chosen to ensure a bistable system, and thus, critical behaviour around threshold values.

Bifurcation diagrams, constructed using XPPAUT, are shown in Figure 2. The fold bifurcation at $D = D_c$ (≈ 0.5853) is a common feature of bistable systems, and acts as the 'tipping point' for the Haldane model. For low dilution rates, the tank settles at an equilibrium with high product concentration, but low overall output ($\mathcal{E}_1$). It is clearly desirable to have a higher dilution rate since the product output Ψ is directly proportional. However for dilution rates D close to D_c, the system is at risk of process noise fluctuations knocking it into the "washed-out" state ($\mathcal{E}_2$), where cell biomass completely dissipates. In order to optimise product output, but not risk a critical transition, the proposed EWS may be of great use.

2.2 Model II : A Mutating Autocatalator

The second model we work with concerns autocatalytic reactions in which an autocatalyst undergoes a mutation process as presented in [10]. It has been selected for its contrasting properties to the Haldane model. The reaction scheme is given by

$$\begin{aligned}
\mathrm{S} + 2\,\mathrm{A} &\xrightarrow{\mathrm{k}_1} 3\,\mathrm{A} && \textit{(A replication)}\\
\mathrm{A} &\xrightarrow{\mathrm{k}_2} \mathrm{U}_1 && \textit{(A decay)}\\
\mathrm{S} + 2\,\mathrm{A} &\xrightarrow{\alpha\mathrm{k}_1} 2\,\mathrm{B} + \mathrm{A} && \textit{(A mutation to B)}\\
\mathrm{S} + 2\,\mathrm{B} &\xrightarrow{\beta\mathrm{k}_1} 3\,\mathrm{B} && \textit{(B replication)}\\
\mathrm{B} &\xrightarrow{\beta/\mathrm{k}_2} \mathrm{U}_2 && \textit{(B decay)}
\end{aligned}$$

where S, A and B refer to the concentrations of substrate, desired product and mutant respectively. Parameters and variable names are displayed in Table 2. This scheme was originally used as a toy model for the formation of cancerous cells from healthy, reproducing cells. Of course, this was a drastic simplification, however it served as an initial step towards modelling the mutation process.

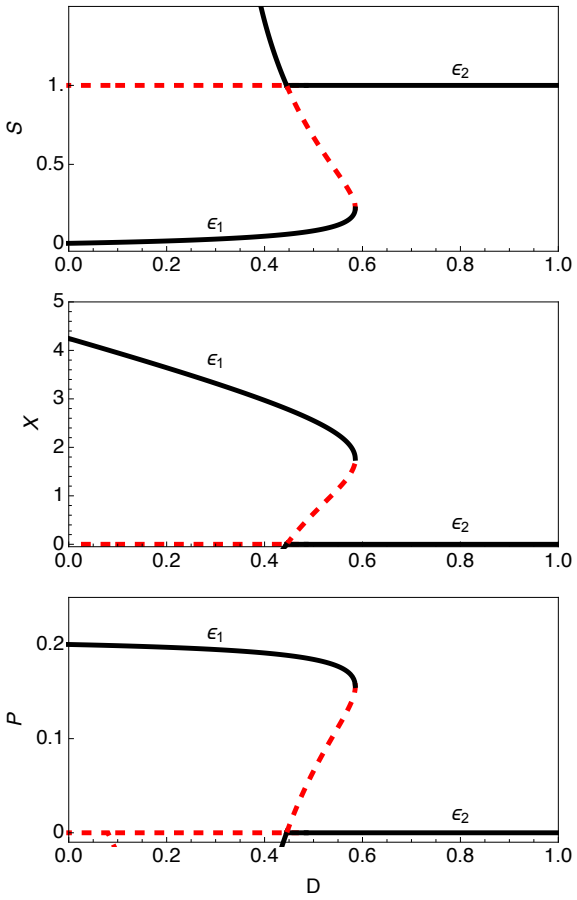

Figure 2: Bifurcation diagrams for the Haldane Model. The fold bifurcation at $D = 0.5853$ permits critical transitions from a functioning bioprocess ($\mathcal{E}_1$) to a 'washed-out' state ($\mathcal{E}_2$). Solid black / dashed red lines represent stable / unstable equilibria.

Notation	Definition
S	Substrate concentration $(mass/vol)$
S_f	Feed substrate concentration $(mass/vol)$
A	Desired product concentration $(mass/vol)$
A	Concentration of desired product in feed $(mass/vol)$
B	Mutant concentration $(mass/vol)$
U_1, U_2	Decomposition product concentrations $(mass/vol)$
k_1, k_2	Rate constants $(time^{-1})$
α	Mutation coefficient $(dimless)$
β	Mutation efficiency $(dimless)$
q	Dilution rate $(time^{-1})$
$\theta = 1/q$	Resident time in reactor $(time)$

Table 2: Symbol definitions for the Mutating Autocatalator Model

With mass action kinetics, the system is described by the set of ordinary differential equations

$$\frac{dS}{dt} = q(S_f - S) - k_1 S A^2 - \alpha k_1 S A^2 - \beta k_1 S B^2, \tag{2.7}$$

$$\frac{dA}{dt} = q(A_f - A) + k_1 S A^2 - \alpha k_1 S A^2 - k_2 A, \tag{2.8}$$

$$\frac{dB}{dt} = -qB + \beta k_1 S B^2 + 2\alpha k_1 S A^2 - \frac{k_2}{\beta} B. \tag{2.9}$$

We work with a dimensionless version of this system, which can be found, along with parameter values, in Appendix A.2. The authors [10] explore the dependence of the system structure on parameter values α and β. We work with one such set of parameter values, that give rise to a Hopf bifurcation at $\theta = \theta_c$ $(= 0.4)$, as illustrated in the bifurcation diagram (Figure 3). From a practical point of view, a rapidly oscillating output is undesirable, and so the system should be kept with $\theta < \theta_c$. We investigate the use of EWS for indication of an upcoming Hopf bifurcation.

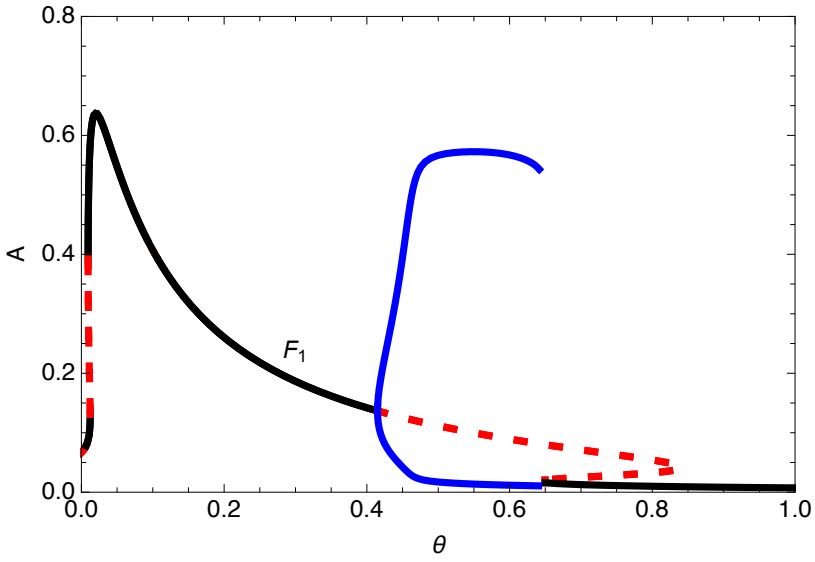

Figure 3: Bifurcation diagram in A for the Mutating Autocatalator Model. The Hopf bifurcation at $\theta = 0.4$ results in a transition from stable behaviour about the equilibrium $\mathcal{F}_1$, to rapid oscillations. Solid black / dashed red lines represent stable / unstable equilibria. The blue line represents a stable limit cycle.

2.3 Ornstein-Uhlenbeck Expressions for EWS

We can use theory from stochastic processes [11] to gain insight into which variables provide the most prominent signals. Analytical expressions may be obtained assuming that stochasticity is incorporated via additive Gaussian-distributed white-noise. Such a system, with state variable $\boldsymbol{x}$ takes the form

$$\frac{d\boldsymbol{x}}{dt} = \boldsymbol{f}(\boldsymbol{x}(\boldsymbol{t})) + B\boldsymbol{\xi}(t) \tag{2.10}$$

where $\boldsymbol{\xi}(t)$ is a vector of independent, zero-mean, Gaussian-distributed white noise sources, thus satisfying

$$\langle \boldsymbol{\xi}(t) \rangle = 0, \quad \langle \xi_m(t)\xi_n(t') \rangle = \delta_{mn}\delta(t-t'). \tag{2.11}$$

Here, δ_{mn} is the Kronecker delta, $\delta(.)$ is the Dirac-delta function, and $< . >$ represents the ensemble mean over time. The matrix B determines noise intensities, and assuming no cross correlation, is diagonal.

Small fluctuations about a stable state gives rise to dynamics that may be approximated by the local linearisation

$$d\boldsymbol{\epsilon}(t) = -A\boldsymbol{\epsilon}(t)dt + Bd\boldsymbol{W}(t) \tag{2.12}$$

where A is the negated Jacobian matrix and $d\boldsymbol{W}(t)$ is a vector of independent, incremental Wiener processes. The stochastic differential equation (2.12), takes the form of a multivariate Ornstein-Uhlenbeck Process, which has many analytically tractable properties [11].

Of particular relevance to EWS is the covariance matrix Σ, of the stochastic process $\boldsymbol{\epsilon}(t)$, defined as the matrix whose (i, j) entry is the covariance

$$\Sigma_{ij} = \mathrm{Cov}(\epsilon_i, \epsilon_j). \tag{2.13}$$

Using the stochastic integral of (2.12) and properties of the Wiener process, Σ can be shown to satisfy

$$A\Sigma + \Sigma A^T = BB^T, \tag{2.14}$$

the continuous Lyapunov equation. We solve this for Σ using 'LyapunovSolve' in *Mathematica* version 10. The lag-τ autocorrelation matrix for the OU process can then be calculated using

$$G(\tau) = e^{-A\tau}\Sigma. \tag{2.15}$$

We caution that these expressions are reliable only in a small neighbourhood of the steady state, since they are derived from the linearised system (2.12). Their applicability is therefore restricted to systems with relatively weak noise. They also require system stationarity (time independent mean) which is satisfied so long as our system is in equilibrium, and control parameters are varied slowly.

Once the best candidates for EWS are established, we test them directly on simulated data, using methodology outlined below.

2.4 Testing EWS on Simulated Data

We simulate the two models with additive Gaussian white noise to capture the effects of process stochasticity. Stochastic simulation is executed using the MATLAB package 'SDETools'.

To obtain the stationary variance and autocorrelation from simulated time-series data, it is first necessary to eliminate any trends that may arise from evolution of the equilibrium point. We detrend the data using Nadarya Watson estimator with Gaussian kernel at a bandwidth selected based on 'Silverman's rule of thumb' [12]. The smoothed time-series is then subtracted from the raw data, to obtain the residual time-series, which we use to calculate the statistical indicators. Variance and lag-1 autocorrelation are calculated over a rolling window of 40% the length of the time-series using a package in *R* [13]. This procedure is illustrated with a simulation of the Haldane model in Figure 6.

3 Results

We check the validity of the proposed EWS for the models reviewed in 'Methods'. We compute the OU expressions for variance and autocorrelation to determine which state variable should give the most prominent signals, and then demonstrate their application to simulated time-series of trajectories approaching a critical transition.

3.1 Model I : The Haldane Model

Recall that the Haldane system transitions from the functioning state $\mathcal{E}_1$ to the highly undesirable 'washed-out' state $\mathcal{E}_2$ if the dilution rate exceeds the threshold value D_c. We simulate this transition by slowly increasing D beyond D_c as in Figure 4.

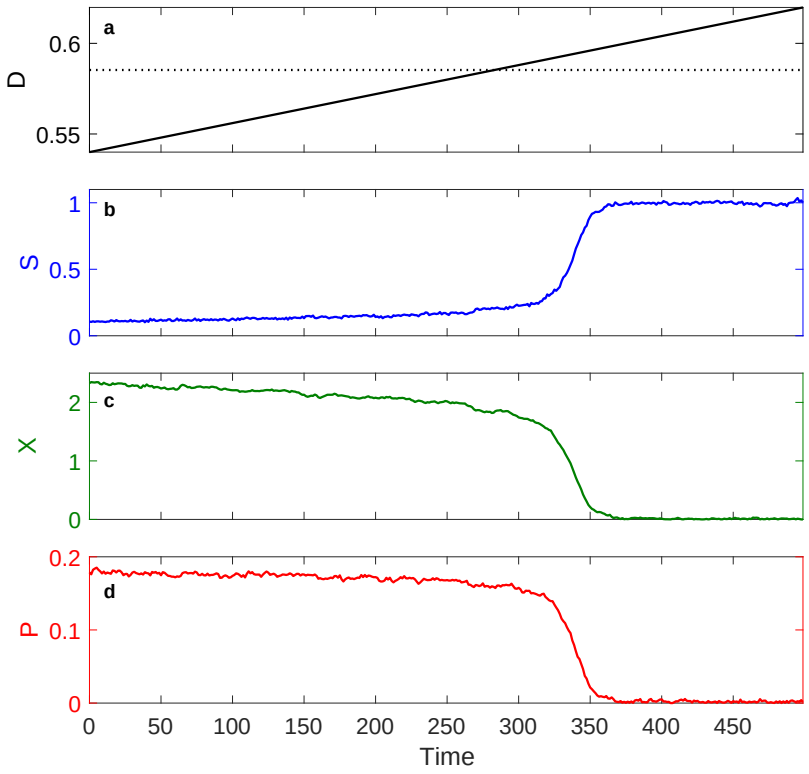

Figure 4: **a)** Dilution rate D (solid line) increasing linearly past fold bifurcation point (dashed line). **b-d)** Time series of substate S, cell X, and product P concentrations as D increases as in a.

To compute the OU expressions for autocorrelation and variance about the steady state $\mathcal{E}_1$, we evaluate the Jacobian matrix at $\mathcal{E}_1$ and solve the continuous Lyapunov equation (see Methods). The coefficient of variation (variance upon mean) and lag-1 autocorrelation for each state variable are plotted in Figure 5. We see that the statistics in S undergo significant increase in the approach to the transition, and so should serve as a prominent EWS.

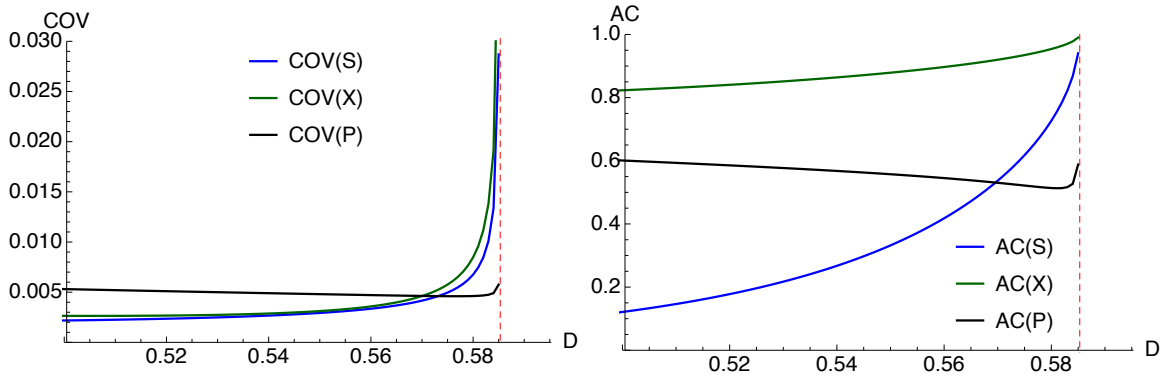

Figure 5: Coefficient of variation (left) and lag-1 autocorrelation (right) of the Ornstein-Uhlenbeck process localised at $\mathcal{E}_1$, as D approaches the fold bifurcation.

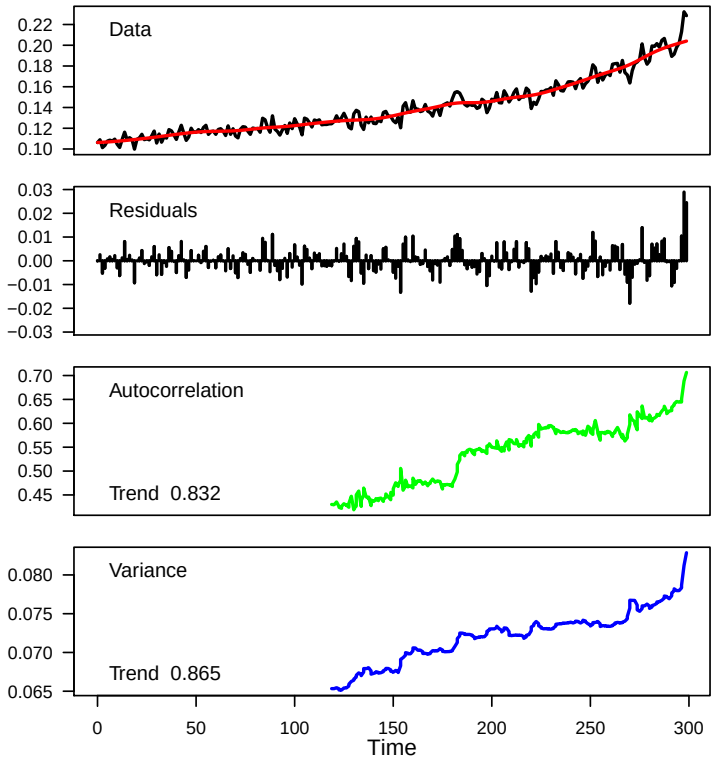

Figure 6: **Data:** Time-series data for S is detrended to remove any non-stationary behaviour. **Residuals** are calculated as the difference between the data and the smoothed curve. **Autocorrelation** and **variance** are calculated over a rolling window with length 40% of the full time-series.

When running simulations, we find this is indeed the case. Computing the EWS from residual time-series' (Figure 6) we find a strong increasing trend in both variance and autocorrelation. Figure 7 shows the statistical indicators of autocorrelation and variance computed from multiple stochastic trajectories, in their pre-transition phase.

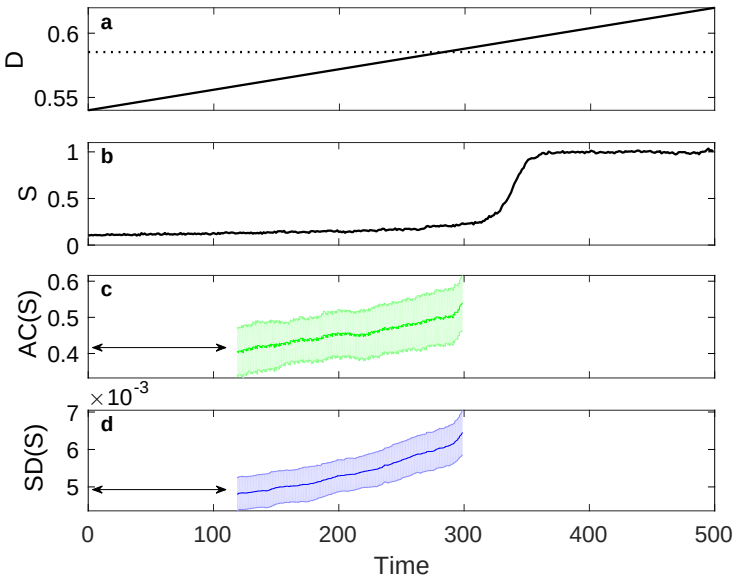

Figure 7: **a)** Dilution rate D (solid line) increasing linearly past fold bifurcation point (dashed line). **b)** Substrate concentration as D increases as in a. **c)** Lag-1 autocorrelation of the residual substrate time series in b (black line shows mean AC, shaded regions shows two standard deviations of 200 stochastic realisations using different random number seeds). **d)** Standard deviation of the residual substrate time series (same format as c). Approach to computing these indicators is outlined in Methods section.

3.2 Model II : The Mutating Autocatalator

We apply the same procedure to the Mutating Autocatalator model. The OU expressions for the coefficient of variation and lag-1 autocorrelation about the equilibrium $\mathcal{F}_1$ are plotted in Figure 8. Interestingly, the system tends towards becoming perfectly anti-correlated as the Hopf bifurcation is approached. This is a surprising, but exciting result since this discrepancy with fold bifurcations could provide a way distinguish upcoming transitions in systems with unknown stability structure. Though proven to become more correlated in one-dimensional systems [6] interactions in multi-variable systems can have significant effects on EWS. This, in itself, is an exciting and important area of research.

These EWS are verified with multiple simulations of the system approaching the Hopf bifurcation, as shown in Figure 9.

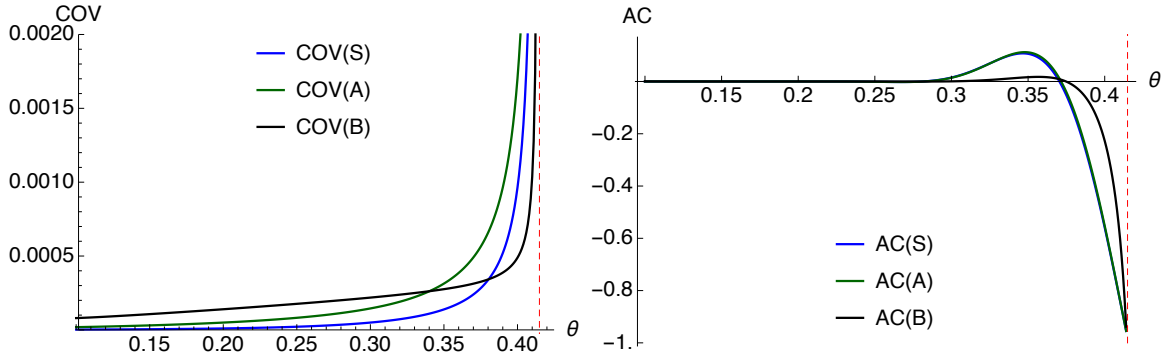

Figure 8: Coefficient of variation (left) and lag-1 autocorrelation (right) of the Ornstein-Uhlenbeck process localised at $\mathcal{F}_1$, as θ approaches the Hopf bifurcation.

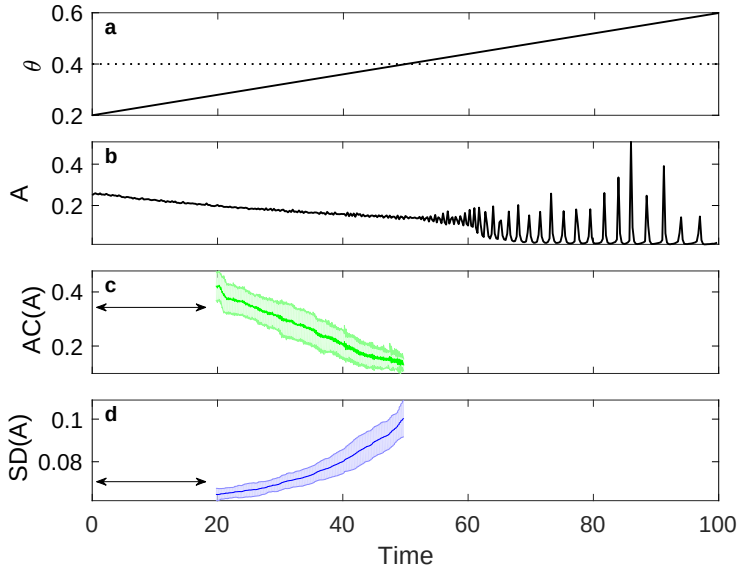

Figure 9: **a)** Resident time in reactor θ (solid line) increasing linearly past Hopf bifurcation (dashed line). **b)** Cell concentration as θ increases as in a. **c)** Lag-1 autocorrelation of the residual substrate time series in b (bold line shows mean AC, shaded regions show two standard deviations of 200 stochastic realisations using different random number seeds). **d)** Standard deviation of the residual substrate time series (same format as c). Computation of indicators is outlined in Methods section.

4 Discussion

A new approach in the field of chemical engineering has been suggested for the careful monitoring of continuous bioprocesses at risk of undesirable transitions. The bifurcation analysis of a simple model showed that product output is maximised for a parameter configuration that puts the system at high-risk of an irreversible transition to a 'washed-out' state. To achieve a safe-operating regime while at the same time yielding high output, the proposed early warning signals could be of significant use.

This paper has applied the basics of critical transition theory to simple models, the tip of what could potentially be a large ice-berg. Much work needs to be done before justifying their application to commercial systems, such as testing in more complex models, and verification in lab experiments. Should the measurement of early warning signals in real bioprocesses prior to transition be successful, this could become an important area of research.

In addition to the EWS described in this paper, there are other metric and model-based indicators that have shown promise [14, 15, 16]. Approaches are also being developed for systems where the underlying mechanisms are predominantly unknown [19, 20]. The literature on EWS in complex systems is growing fast, and due to their generic nature, we anticipate that they may find themselves in new disciplines to come.

We hope that this paper brings awareness to EWS as a potential tool in the field of chemical engineering, and encourages further work with regards to their application.

References

[1] Kazuyuki Shimizu. A tutorial review on bioprocess systems engineering. *Computers & chemical engineering*, 20(6-7):915–941, 1996.

[2] A Uppal, WH Ray, and AB Poore. On the dynamic behavior of continuous stirred tank reactors. *Chemical Engineering Science*, 29(4):967–985, 1974.

[3] A Ajbar. Classification of static behavior of a class of unstructured models of continuous bioprocesses. *Biotechnology progress*, 17(4):597–605, 2001.

[4] Steven H Strogatz. *Nonlinear dynamics and chaos: with applications to physics, biology, chemistry, and engineering*. Westview press, 2014.

[5] Marten Scheffer, Jordi Bascompte, William A Brock, Victor Brovkin, Stephen R Carpenter, Vasilis Dakos, Hermann Held, Egbert H Van Nes, Max Rietkerk, and George Sugihara. Early-warning signals for critical transitions. *Nature*, 461(7260):53–59, 2009.

[6] C Wissel. A universal law of the characteristic return time near thresholds. *Oecologia*, 65(1):101–107, 1984.

[7] Vasilis Dakos, Stephen R Carpenter, Egbert H van Nes, and Marten Scheffer. Resilience indicators: prospects and limitations for early warnings of regime shifts. *Philosophical Transactions of the Royal Society B: Biological Sciences*, 370(1659):20130263, 2015.

[8] TK Ghose and RD Tyagi. Rapid ethanol fermentation of cellulose hydrolysate. ii. product and substrate inhibition and optimization of fermentor design. *Biotechnology and Bioengineering*, 21(8):1401–1420, 1979.

[9] AF Rozich, AF Gaudy, and PC D'adamo. Selection of growth rate model for activated sludges treating phenol. *Water Research*, 19(4):481–490, 1985.

[10] AE Abasaeed. Bifurcation and chaos for a mutating autocatalator in a cstr. *Bioprocess and Biosystems Engineering*, 22(4):337–346, 2000.

[11] Crispin W Gardiner et al. *Handbook of stochastic methods*, volume 3. Springer Berlin, 1985.

[12] Bernard W Silverman. *Density estimation for statistics and data analysis*, volume 26. CRC press, 1986.

[13] Vasilis Dakos, Stephen R Carpenter, William A Brock, Aaron M Ellison, Vishwesha Guttal, Anthony R Ives, Sonia Kéfi, Valerie Livina, David A Seekell, Egbert H van Nes, et al. Methods for detecting early warnings of critical transitions in time series illustrated using simulated ecological data. *PloS one*, 7(7):e41010, 2012.

[14] Vishwesha Guttal and Ciriyam Jayaprakash. Changing skewness: an early warning signal of regime shifts in ecosystems. *Ecology letters*, 11(5):450–460, 2008.

[15] Vasilis Dakos, Sarah Glaser, Chih-hao Hsieh, and George Sugihara. Elevated nonlinearity as indicator of transition to overexploitation in fish stocks. *bioRxiv*, page 051532, 2016.

[16] David A Seekell, Stephen R Carpenter, and Michael L Pace. Conditional heteroscedasticity as a leading indicator of ecological regime shifts. *The American Naturalist*, 178(4):442–451, 2011.

[17] Vasilis Dakos, Marten Scheffer, Egbert H van Nes, Victor Brovkin, Vladimir Petoukhov, and Hermann Held. Slowing down as an early warning signal for abrupt climate change. *Proceedings of the National Academy of Sciences*, 105(38):14308–14312, 2008.

[18] Stephen R Carpenter, Jonathan J Cole, Michael L Pace, Ryan Batt, WA Brock, Timmothy Cline, Jim Coloso, James R Hodgson, Jim F Kitchell, David A Seekell, et al. Early warnings of regime shifts: a whole-ecosystem experiment. *Science*, 332(6033):1079–1082, 2011.

[19] Steven J Lade and Thilo Gross. Early warning signals for critical transitions: a generalized modeling approach. *PLoS Comput Biol*, 8(2):e1002360, 2012.

[20] William A Brock and Stephen R Carpenter. Early warnings of regime shift when the ecosystem structure is unknown. *PLoS One*, 7(9):e45586, 2012.

A Model Rescaling and Parameter Values

A.1 The Haldane Model

The Haldane Model given in Section 2.1 can be non-dimensionalised [3] with the rescaling

$$\bar{S} = \frac{S}{S_f}, \quad \bar{X} = \frac{aX}{S_f}, \quad \bar{P} = \frac{P}{K_{1P}}, \quad \bar{D} = \frac{D}{\mu_1}, \quad \bar{t} = \mu_1 t, \quad \bar{\mu} = \frac{\mu}{\mu_1}, \quad \bar{\epsilon} = \frac{\epsilon}{\mu_2}, \tag{A.1}$$

to give

$$\frac{dS}{dt} = D(1-S) - \left(\frac{S}{\beta_2 + S + \gamma_2 S^2}\right)\frac{\lambda_1}{1+\lambda_3 P}X, \tag{A.2}$$

$$\frac{dX}{dt} = \left(\frac{S}{\beta_1 + S + \gamma_1 S^2}\right)\frac{1}{1+P}X - DX, \tag{A.3}$$

$$\frac{dP}{dt} = \left(\frac{S}{\beta_2 + S + \gamma_2 S^2}\right)\frac{\lambda_2}{1+\lambda_3 P}X - DP, \tag{A.4}$$

where

$$\beta_i = \frac{K_{iS}}{S_f}(i=1,2), \quad \gamma_i = \frac{S_f}{K_{i1}}(i=1,2), \quad \lambda_1 = \frac{\mu_2}{\mu_1}, \quad \lambda_2 = \frac{\mu_2 S_f}{a\mu_1 K_{1P}}, \quad \lambda_3 = \frac{K_{1P}}{K_{2P}}. \tag{A.5}$$

Model parameter values used throughout this paper are given in the Table 3.

Dimensionless parameter	Value
β_1	0.0471
γ_1	1.2
β_2	0.1
γ_2	1
λ_1	0.5
λ_2	0.1
λ_3	1

Table 3: Dimensionless parameter values for the Haldane Model

A.2 The Mutating Autocatalator Model

The Mutating Autocatalator Model in Section 2.2 can be non-dimensionalised [10] with the rescaling

$$\bar{S} = \frac{S_f - S}{S_f}, \quad \bar{A} = \frac{A}{S_f}, \quad \bar{B} = \frac{B}{S_f}, \tag{A.6}$$

to obtain

$$\frac{d\bar{S}}{dt} = -\frac{\bar{S}}{\theta} + (1+\alpha)\gamma_1(1-\bar{S})\bar{A}^2 + \beta\gamma_1(1-\bar{S})\bar{B}^2, \tag{A.7}$$

$$\frac{d\bar{A}}{dt} = \frac{\bar{A}_f - \bar{A}}{\theta} + (1-\alpha)\gamma_1(1-\bar{S})\bar{A}^2 - \gamma_2\bar{A}, \tag{A.8}$$

$$\frac{d\bar{B}}{dt} = \frac{\bar{B}_f - \bar{B}}{\theta} + \beta\gamma_1(1-\bar{S})\bar{B}^2 + 2\alpha\gamma_1(1-\bar{S})\bar{A}^2 - \frac{\gamma_2}{\beta}\bar{B}, \tag{A.9}$$

where

$$\gamma_1 = k_1 S_f^2, \quad \gamma_2 = k_2, \quad \theta = \frac{1}{q} \tag{A.10}$$

In this paper we take parameter values as in Table 4.

Dimensionless parameter	Value
γ_1	450
γ_2	11.25
$\bar{A}_f$	0.067
α	0.05
β	0.8

Table 4: Dimensionless parameter values for the Mutating Autocatalator Model